The Mechanism of Cure of Tetraglycidyl Diaminodiphenyl Methane with Diaminodiphenyl Sulfone

A. GUPTA, M. CIZMECIOGLU, D. COULTER, R. H. LIANG, A. YAVROUIAN, F. D. TSAY, and J. MOACANIN, *Jet Propulsion Laboratory, California Institute of Technology, Pasadena, California 91109*

Synopsis

The curing reaction of tetraglycidyl diaminodiphenyl methane (TGDDM) with diaminodiphenyl sulfone (DDS) has been investigated using differential scanning calorimetry, Fourier transform IR spectroscopy, and ESR spin trapping techniques. A mechanism has been proposed, and the cure kinetics has been obtained at 177°C. The major conclusion is that cure proceeds mainly through chain extension, while crosslinking occurs through the reaction of hydroxyl groups with epoxides, resulting in formation of ether linkages.

INTRODUCTION

Investigations into the cure kinetics of the tetraglycidyl diaminodiphenyl methane–diaminodiphenyl sulfone (TGDDM—DDS) resin system may be broadly categorized as being aimed either at understanding the mechanism and rate of change of physical properties (e.g., viscosity, loss modulus) during cure[1–5] or at developing a numerical model which can be used to monitor and control the curing process in industrial situations.[6] Studies in the fundamental aspects of the chemistry have always used the time–temperature–transformation (TTT) type of diagrams as a referent, in part because the curing reaction is expected to be quenched by the process of vitrification.[7] In this part of a continuing series of reports on investigations of chemical kinetics of the cure of the TGDDM–DDS system,[8,9] we outline our preliminary conclusions on the structures of the more numerous network junction points (some of which might be crosslinks) and the rates of their formation under isothermal conditions. We have investigated epoxide–epoxide reactions using ESR spin traps, relative reactivity of epoxide groups to hydroxyl and primary amine groups, and the importance of reaction of secondary amines (formed by epoxide-primary amine reactions) with epoxides under certain commonly used curing conditions.

The chemical kinetics of a complex viscous reactive system may be characterized by different rate limiting processes at different stages of cure, conversion, viscosity, and temperature. One may use a simplified diagram as shown in Figure 1 to describe the dependence of the net activation energy to conversion and temperature, assuming that a homogenous (but not necessarily unique) network is formed. Superimposed on it would be the controlling effect of viscosity, especially at the vicinity of the glass transition temperature of the system, which is itself a function of chemical composition and temperature. This picture tends

Journal of Applied Polymer Science, Vol. 28, 1011–1024 (1983)
 CCC 0021-8995/83/031011-14$02.40

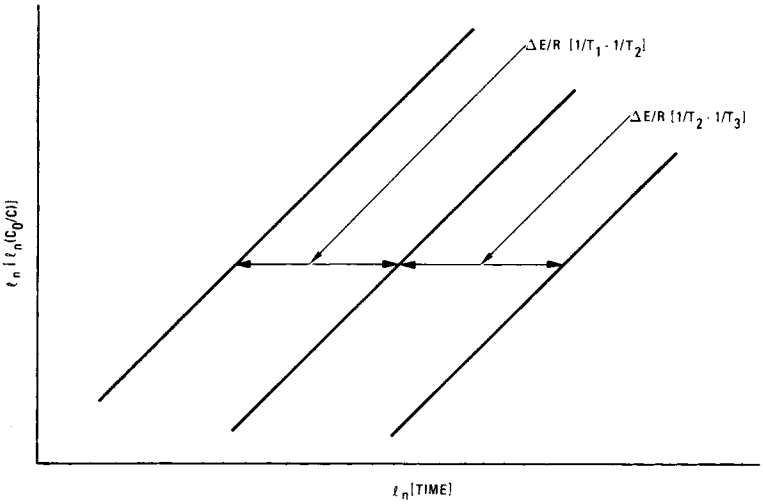

Fig. 1. Schematic representation of time–temperature conversion dependence of the reaction rate.

to overlook the effect of the preexponential or frequency factor, which is ultimately controlled by the molecularity of reactions. The order of reaction in a condensed phase is determined both by diffusion-controlled transport of reactive groups and statistical distribution of distances between reactive groups as it exists in the medium at any moment. An analogous situation arises in the fast quenching of electronically excited states in condensed media which is best described by a combination of "static quenching" processes and a diffusion controlled quenching process, the Stern–Volmer kinetics.[10] The static processes may dominate in a highly viscous medium, causing the overall reaction to appear pseudo zeroth order for both reactants.

EXPERIMENTAL

A commercial grade of tetraglycidyl diaminediphenyl methane (TGDDM), namely, MY720 supplied by Ciba Geigy, was used as received. Diaminodiphenyl sulfone (DDS) was recrystallized twice to form off-white needles. *N,N'*-dimethyldiphenyl sulfone (DMDDS) was synthesized as follows: 31.7 g (0.1 mol) of 4,4'-dichlorodiphenyl sulfone, 62 mL of 60% aqueous methyl amine, and 5 g of Cu_2Cl_2 were heated at 220°C for 24 h in a high pressure bomb. The reaction product was then dissolved in boiling ethanol, treated with charcoal, and filtered through celite. The product was isolated from the ethanol solution after cooling overnight at −10°C and recrystallized from ethanol one more time. The yield was 52%, and the product has a melting point at 173°C. The results of the elemental analysis, as determined experimentally, are: C, 61.00%; H, 5.85%; N, 10.21%; S, 11.80%. The NMR and IR spectra of DMDDS are shown in Figure 2. The synthetic scheme for DMDDS is given in Scheme I.

Chemically pure TGDDM (98–99%) was kindly supplied by Dr. G. Hagenauer of the Army Materials Research Center, Watertown, Mass. Throughout the following discussion, we shall refer to pure TGDDM as TGDDM, while using MY720® for the commercial grade TGDDM.

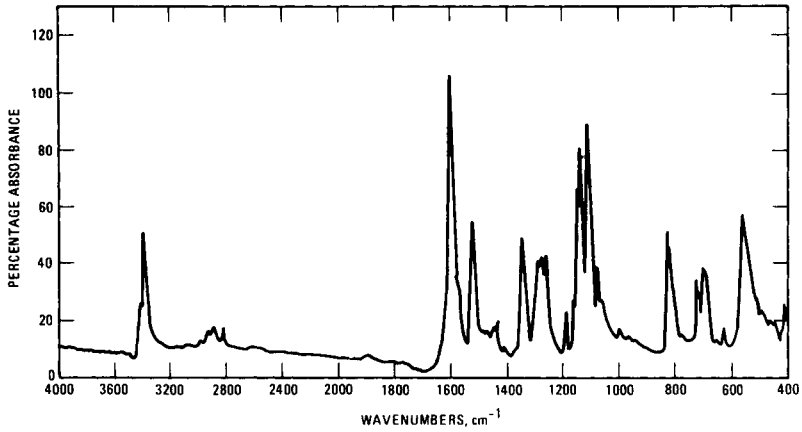

(a)

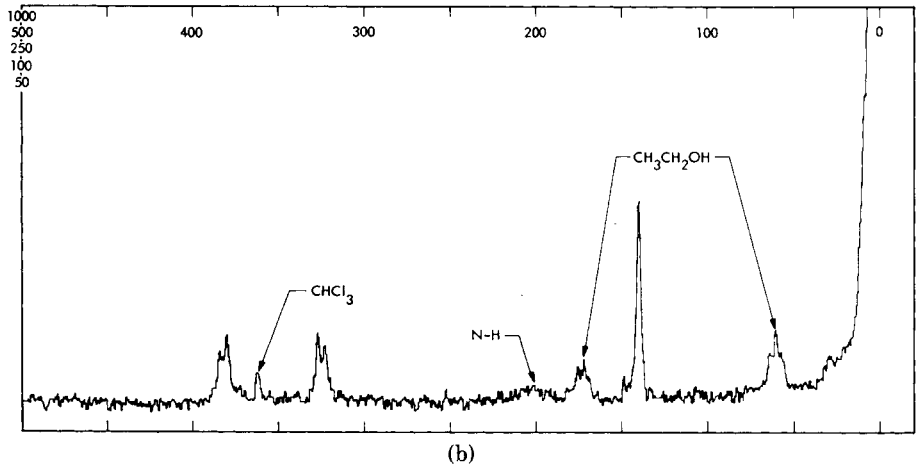

(b)

Fig. 2. Chemical characterization of *N,N'*-dimethylamino diphenylsulfone: (a) IR spectrum, smear on salt flat; (b) NMR spectrum, solvent $CDCl_3$.

Electron Spin Resonance (ESR) Spectroscopy

TGDDM was mixed with 0.1 wt % of *n-tert*-butyl-α-phenylnitrone (PBN), a well-known spin trap, deareated in a ESR tube and placed inside the cavity of a Century Series E-15 ESR spectrometer. The reaction of the spin trap with the epoxide, and the consequent labeling of a random sample of epoxides, is completed within 10–15 min at 140°C. Figure 3 shows typical ESR spectra obtained. These spectra may be resolved into a "narrow" and a "broad" line pattern, which on closer examination was found to have slightly different "*g*" values and hence different hyperfine coupling constants. Table I shows the

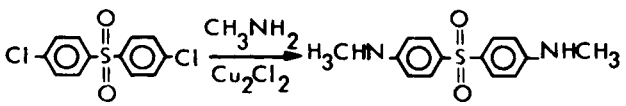

Scheme I.

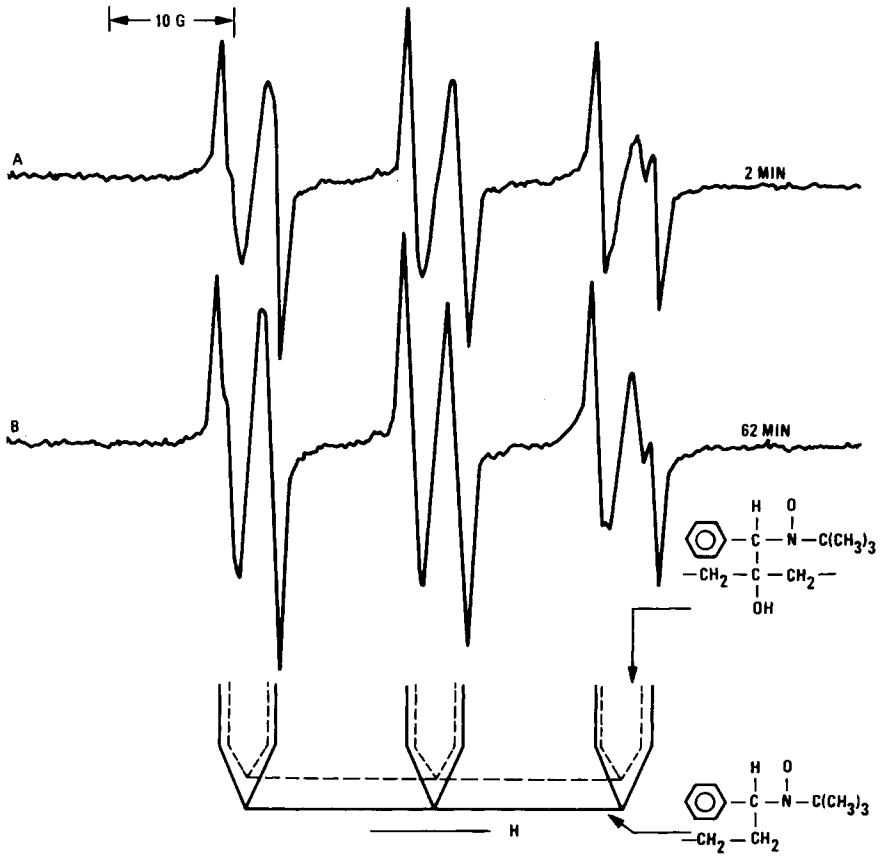

Fig. 3. Assignment of ESR spectra of labelled epoxides in the TGDDM–PBN system; curing temp = 140°C.

nitrogen and proton hyperfine coupling constants determined for these PBN spin adducts.

The line widths of the "narrow" and "broad" components due to —CH_2—CH(OH)—CH_2—S and —CH_2—CH(S)—CH_2OH, when S is spin label, were recorded as a function of time on isothermal cure at 140°C. The molecular rotational times of the "narrow" and "broad" components as determined from the line width are shown in Figure 4. A mixture of TGDDM, DDS (22 wt %), and PBN (0.1 wt %) was made up at 120°C, placed in ESR (quartz) tubes and deareated, as before. Typical spectra on isothermal cure at 140°C are shown in Figure 5. It was found that the broad component due to —CH—CH(S)—CH_2OH is formed initially, and for longer curing periods, a "frozen in *trans*" configuration can be distinguished in which the slow rotation of the spin label segment about the N–C bond causes inhomogenous line broadening. Figure 6 shows a plot of molecular rotational time vs. time at 140°C for the broad component.

Differential Scanning Calorimetry (DSC)

A mixture of MY720 and DDS (containing 22 wt % of DDS) was prepared at 120°C under high purity N_2. This mixture was cured isothermally at 177°C

TABLE I

	SPIN ADDUCT	SPECTRAL LINEWIDTH	HYPERFINE CONSTANT A^N (GAUSS) A^H	
1.	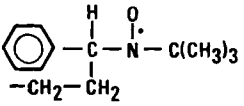	NARROW	15.1	4.4
2.	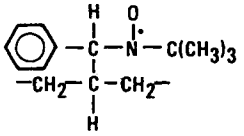	BROAD	14.9	3.3
3.	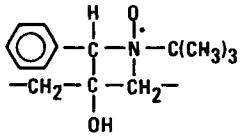	BROAD	14.8	3.1
4.	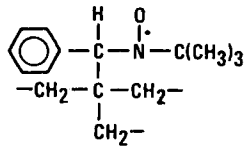	BROAD	14.8	3.1
5.	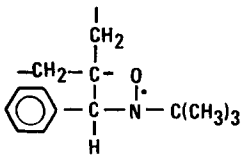	BROAD	15.9	22.6

(350°F) under a positive pressure of N_2 gas. The oven thermostat was controlled by a thermocouple placed inside a metal plate on which the samples were placed. The temperature of the plate was 177° ± 2°C. Samples were withdrawn at 10 time intervals ranging from 10 min to 210 min (3.5 h) and analyzed by differential scanning calorimetry in dynamic mode, scanned at 10°C/min. Table II gives the thermal parameters such as the temperatures at which the exotherms begin and at which they are maximum, as well as the total heat evolved per unit mass of the sample. These measurements indicate that complete cure is never achieved at 177°C. The plot of conversion as measured by the decrease in the area of the exotherm recorded on the above described samples relative to a control sample vs. the isothermal curing period is shown in Figure 7.

Mixtures of MY720, DDS, and DMDDS were prepared as shown in Table III. They were all mixed at the same temperature, and DSC thermograms were recorded at various scanning rates. Figure 8 shows typical thermograms recorded for mixtures containing DDS and DMDDS only. Table III also gives various thermal parameters readily extracted from the DSC data. The observation which can be most readily made from these data is that the heat evolved per unit

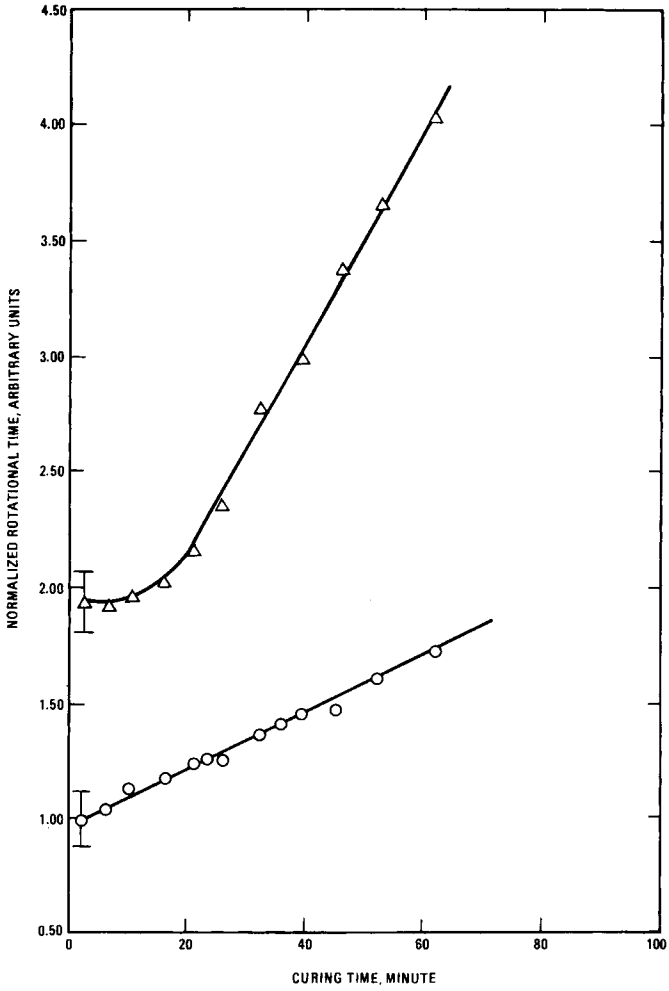

Fig. 4. Plot of normalized rotational correlation times of the spin labels in the TGDDM–PBN system vs. curing time; spectra recorded at 140°C: (△) broad component; (○) narrow component.

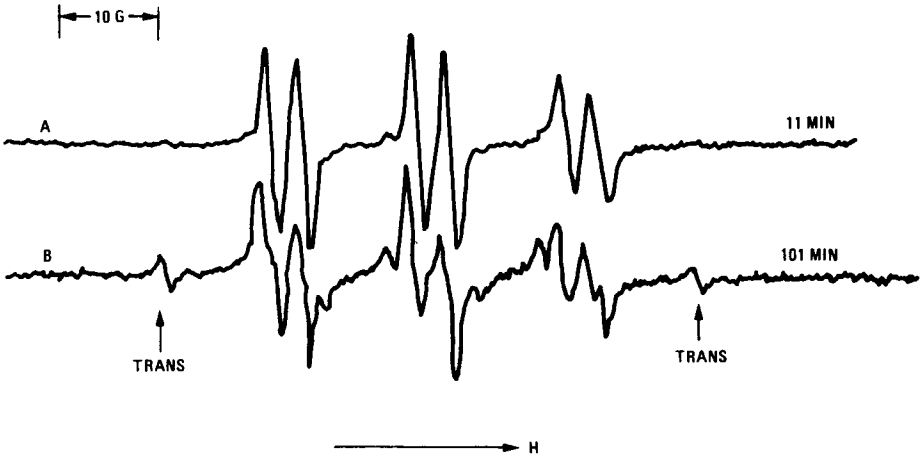

Fig. 5. Typical ESR spectra of the spin labels in the TGDDM–DDS–PBN system; curing temperature = 140°C.

Here the value of m/n for DAP telomer is expected to be 1.33 from the bulk polymerization result,[2] and, moreover, the cyclic structure II is predominantly an 11-membered ring formed via consecutive intramolecular head-to-tail addition of the uncyclized radical.[15] For DAT telomer a large cyclic structure formation leading to around 10% loss of unreacted pendant allyl groups[16] might occur via nonconsecutive intramolecular addition, in which uncyclized radical adds to any other double bond pendant to the chain than to the double bond present in the same monomer unit, although the intramolecular cyclization in the monomeric DAT unit is impossible in view of the molecular model.

Second, for the telomer and/or polymer obtained at a higher conversion when the crosslinking is significant, the structure is complexed depending on the polymerization conditions because the rate of consumption of carbon tetrabromide is fast compared to DAP monomer, leading to the increase of the primary chain length of the telomer produced at a higher conversion, and the crosslinking between the pendant double bond of the telomer and the growing chain radical gradually becomes important with the progress of polymerization, both of which affect the molecular weight distribution of the telomer and/or polymer obtained.

In this connection, the telomer (II) was obtained in 75% yield in the polymerization at $[CBr_4]/[DAP] = 1/3$ as mentioned above; from the analytical results of carbon and bromine contents and molecular weight the structure of the telomer assumed as $(CBr_3)_m(DAP)_nBr_m$ was determined to be $m = 2.48$ and $n = 6.20$, the analytical results being recalculated in a good agreement with the experimental results: molecular weight, 2349; C, 45.65%; Br, 33.74%. Moreover, the number of unreacted pendant allyl groups, i.e., the uncyclized structural units I, was estimated at 3.31 from the iodine value; then, the cyclized units II are calculated to be 1.41 because the number of crosslinked units corresponds to m − 1, i.e., 1.48. These results suggest that the intramolecular cyclization of uncyclized radical in the polymerization of DAP is suppressed in the telomerization, as is evident from the comparison with the bulk polymerization result[2] described above. That is, the extent of cyclization of the telomer may depend on the chain length, i.e., the cyclization be enhanced with increased degree of polymerization. This suggestion is considered quite important for the comprehensive understanding of the cyclopolymerization behavior of nonconjugated dienes; thus the details will be discussed in our subsequent article.[17]

References

1. M. Oiwa and A. Matsumoto, *Progress in Polymer Science Japan*, Kodansha Ltd., Tokyo, 1974, Vol. 7, p. 107.

2. A. Matsumoto, K. Asano, and M. Oiwa, *Nippon Kagaku Zasshi*, **90,** 290 (1969).

3. A. Matsumoto and M. Oiwa, *J. Polym. Sci., A-1,* **8,** 751 (1970).

4. A. Matsumoto and M. Oiwa, *Kogyo Kagaku Zasshi*, **72,** 2127 (1969).

5. A. Matsumoto, S. Yokoyama, T. Kohno, and M. Oiwa, *J. Polym. Sci., Polym. Phys. Ed.*, **15,** 127 (1977).

6. J. Brandrup and E. H. Immergut, *Polymer Handbook*, Wiley-Interscience, New York, 1975.

7. A. A. Vansheidt, G. Khardi, *Acta Chim. Acad. Sci. Hung.*, **20,** 261 (1959); *Chem. Abstr.*, **54,** 6180 (1960).

8. A. Matsumoto, K. Iwanami, and M. Oiwa, *J. Polym. Sci., Polym. Lett. Ed.*, **19,** 497 (1981).

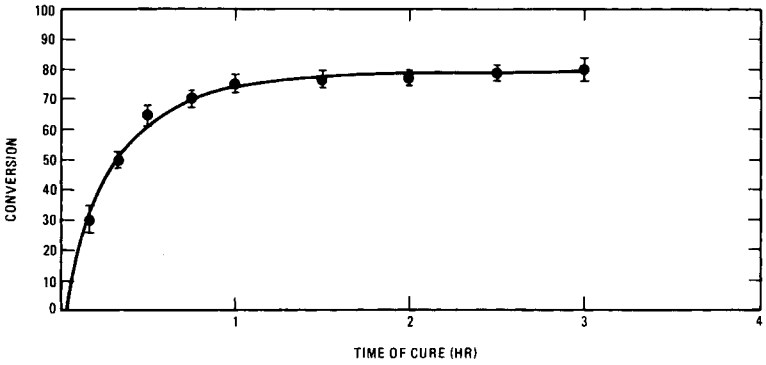

Fig. 7. Plot of conversion vs. curing time for samples isothermally cured at 177°C, as determined from dynamic DSC analysis; scan rate = 10°C/min.

and change in the peak area ratio are also noted in the partially cured samples. FT-IR spectra was also used to monitor the rate of loss of epoxide groups at 905 cm^{-1} and the rate of formation of hydroxyl groups 3400 cm^{-1} as shown in Figures 10(a) and 10(b).

DISCUSSION

The main reactions in the TGDDM–DDS system are shown in Scheme II, each of which is presumably characterized by a different activation energy and preexponential factor. The epoxy–hydroxyl group interaction is probed by the spin trap PBN. The epoxide groups are labelled on reaction of the spin trap with the epoxide group, forming a spin-labeled alcohol (Table I). The increase in the line width of the spin probe is related to increase in the moment of inertia of the segment attached to the spin probe and hence the kinetic chain length of the

TABLE III
DSC Results of Mixtures of MY720 with DDS and DMDDS

Sample no.	MY720 (g)	DDS (g)	DMDDS (g)	Scan rate (°C/min)	Peak temp T_p (°C)	ΔH (J/g)
1	100	28	—	5	254	699
				10	264	597
				20	285	643
				40	310	644
2	100	25.2	2.8	10	270	556
				20	290	567
3	100	21	7	10	276	558
				20	292	589
4	100	14	14	10	281	575
				20	300	564
5	100	7	21	10	286	549
				20	304	563
6	100	—	28	2.5	262	479
				5	276	465
				10	291	575
				20	310	510
				40	328	400

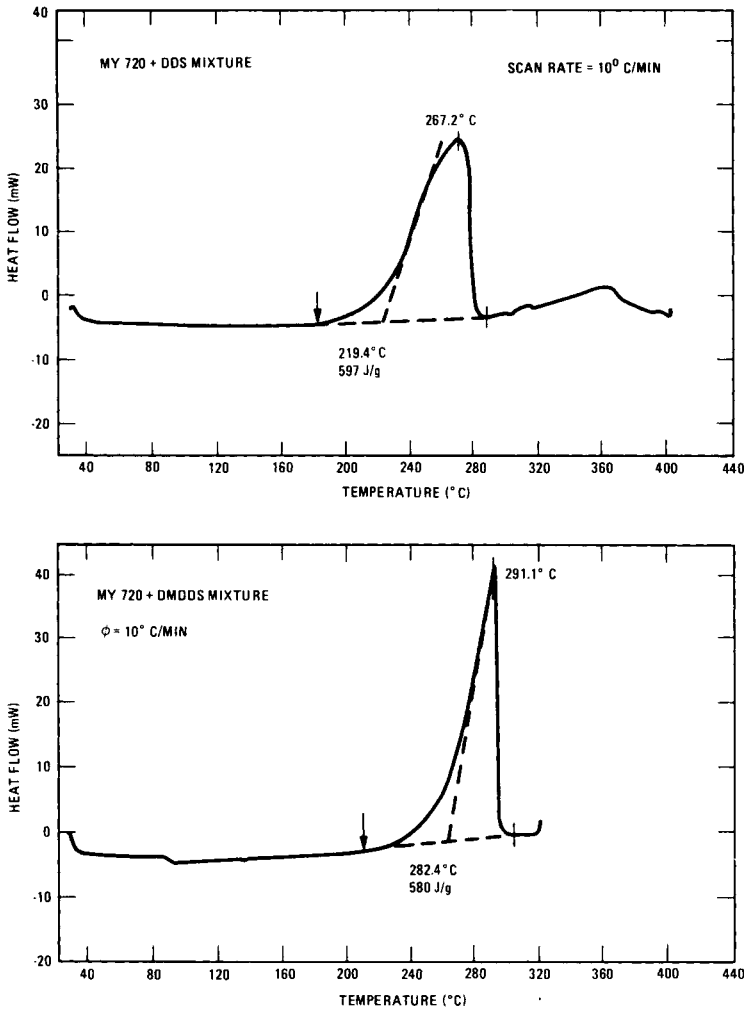

Fig. 8. Typical dynamic DSC thermograms on MY720-DDS and MY720-DMDDS mixtures.

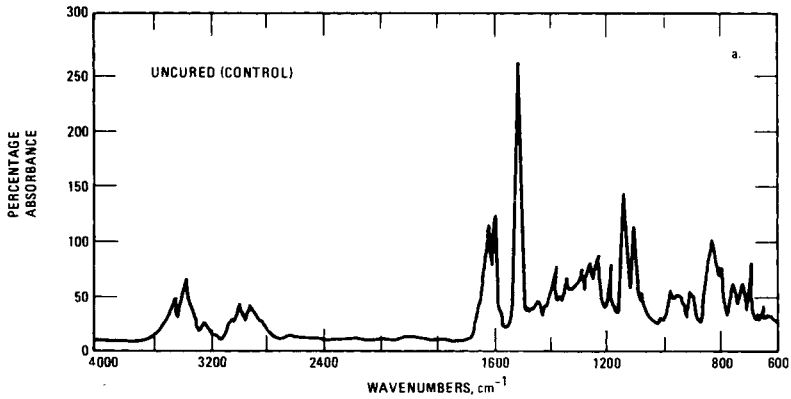

Fig. 9. FT-IR monitoring of isothermal cure of the MY720–DDS system; curing temp = 177°C.

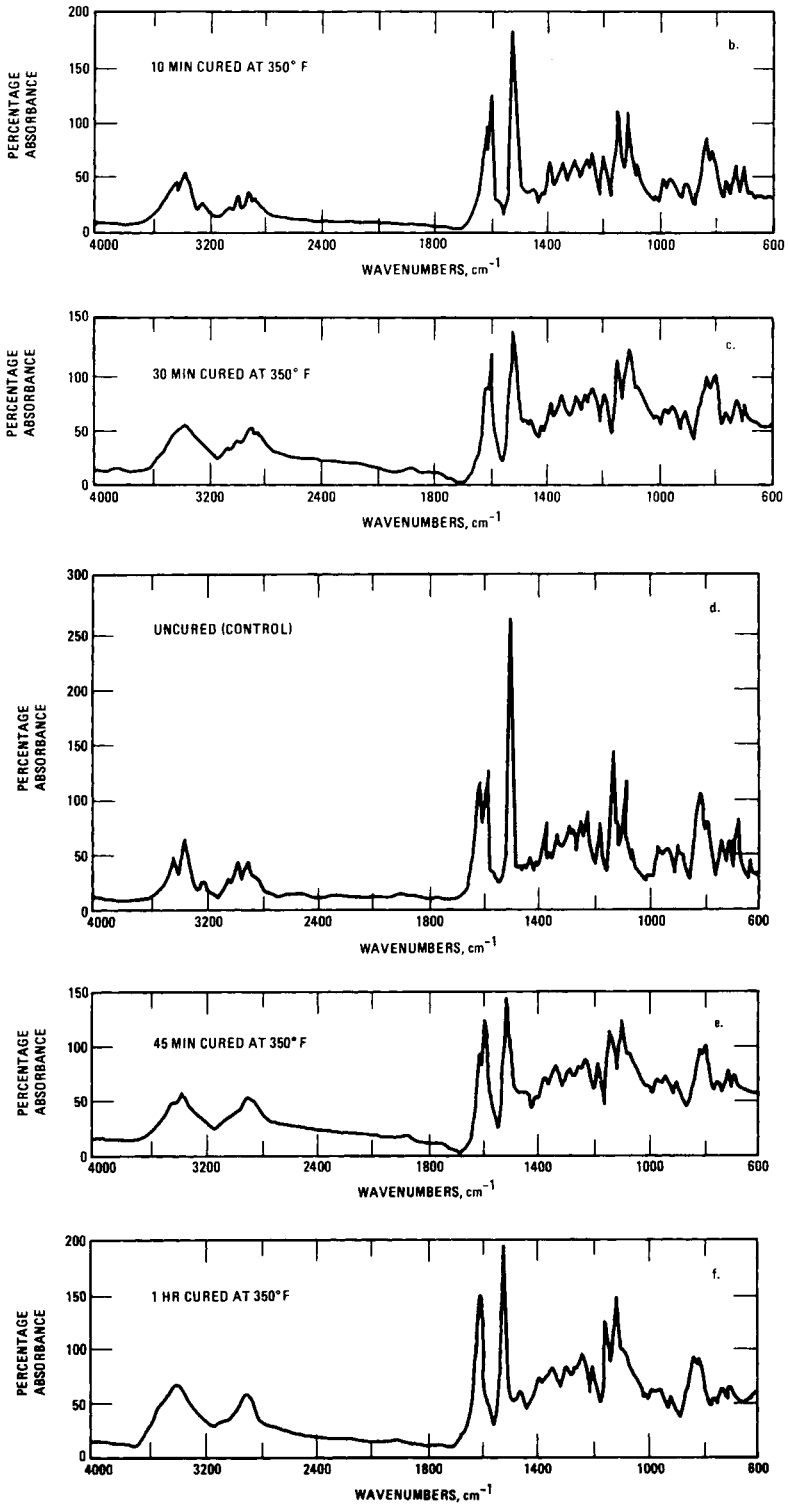

Fig. 9 (*Continued from the previous page.*)

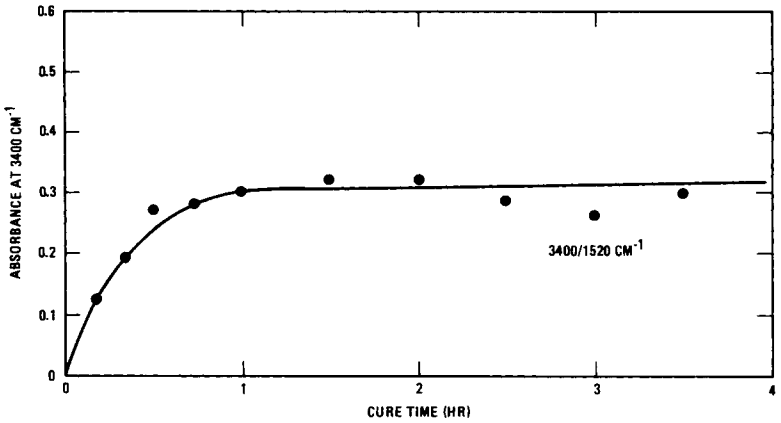

Fig. 10. Plot of absorbance at 3400 cm^{-1} vs. curing time from FT-IR analysis of NY720-DDS mixtures cured isothermally at 177°C.

epoxide-hydroxyl group reaction. Hence the line width data in Figure 3 indicate that the primary alcohol —CH(S)—CH_2OH and the secondary alcohol —CH(OH)—CH_2S have two distinct rates of reaction with epoxide groups, a corollary being that a secondary alcohol cannot generate a primary alcohol upon etherification, as shown in Scheme III. Similarly a primary alcohol always generates another primary alcohol. Thus, if the types and concentrations of hydroxyl groups are known, the structures and rates of formation of ether links formed can be deduced from Figure 4. Since the ratio of rate constants is approximately 10:1, it is clear that steric constraints play a decisive role in determining reactivity in this system even at such an early stage of conversion.

Comparison of the DSC data with the rate of epoxide disappearance data show that while the curing process at 177°C consumes approximately 30% of the epoxide in the first 60 min, heat evolution is approximately 70% complete during

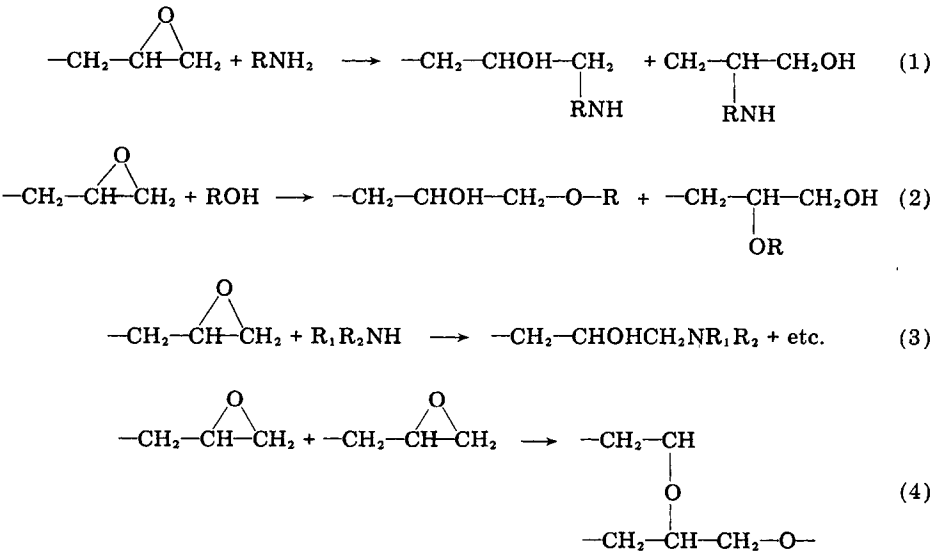

Scheme II.

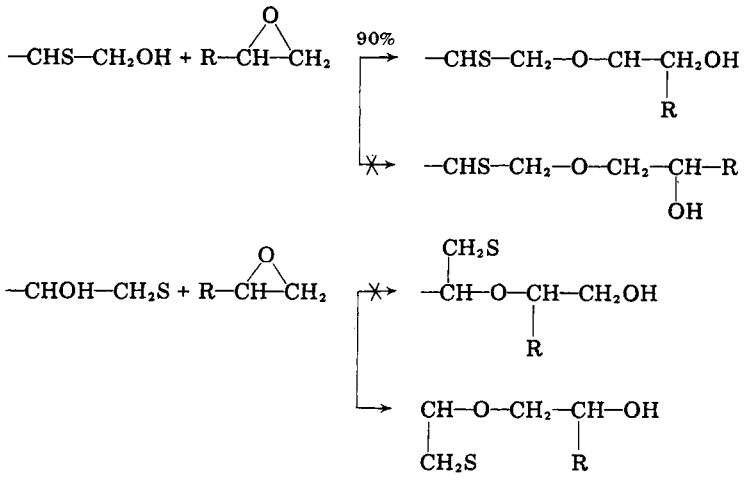

Scheme III.

the same time period, i.e., the epoxide is consumed in two different reactions, one of which is significantly more exothermic than the other, the exothermic reaction dominating the initial curing process at 177°C. Examination of the FT-IR data shows this reaction to be the epoxide–primary amine reaction. The end of this reaction, which culminates in the consumption of a stoichiometric concentration of primary amine, at the end of 60 min at 177°C brings the T_g of the system up to 160–200°C. The concentration of hydroxyl groups and the 1150 cm^{-1}/1105 cm^{-1} peak ratio (secondary amine to primary amine) reaches a plateau at the same time, indicating that the epoxide–secondary amine reaction is not important at 177°C. The same conclusion is reached more rigorously from DSC data on MY720® and DDS/DMDDS mixtures. Data recorded at the same scan rate indicate that the heat evolved per unit mass (and hence unit mole, approximately) of reacting material is the same when DDS is replaced by DMDDS in the curing system. This observation can only be rationalized by assuming that, under the curing conditions of the DSC experiments, DDS acts as a bifunctional curing agent, i.e., the secondary amine formed on curing DDS does not react any further. The lack of reactivity of this secondary amine, which is part of a chain, must be attributed as much to the lack of diffusional transport of the reactive site as to its inaccessibility due to steric hinderence. The secondary amine is presumably involved in the post-curing process at 200°C and above, as observed by Mones and Morgan.[11] TMA analysis and ESR line width analysis (Fig. 6) show that the epoxide–primary amine reaction is quenched and ceases to be the controlling reaction in the cure process when the rising glass transition temperature of the medium exceeds the curing temperature. This change in the major reaction pathway is found to occur at T_g (160–200°C) as measured by thermomechanical analyzer (TMA) analysis on samples cured at 177°C and at 140°C measured by monitoring ESR linewidth on samples cured at 140°C. The plot of line width in Figure 6 indicates that the kinetic chain length of the labeled epoxide (i.e., the labeled alcohol) does not increase any further after 30 min of curing at 140°C. The line width analysis is insensitive to the increase in viscosity of the resin medium beyond this point, until the glass

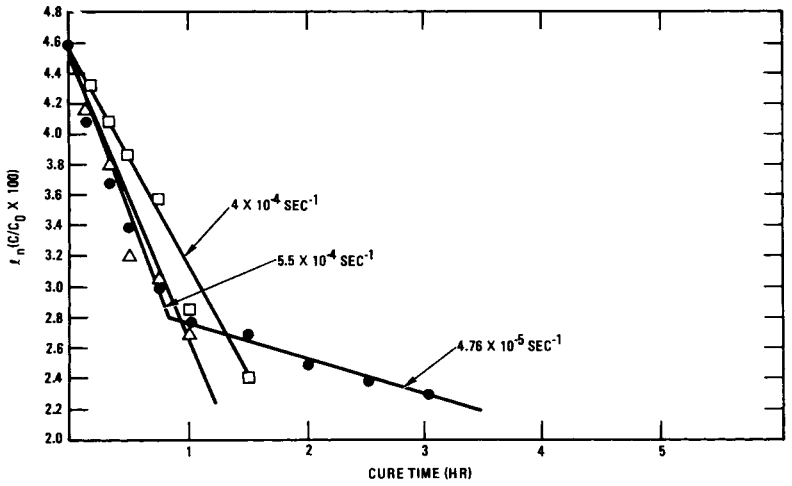

Fig. 11. First order kinetic analysis of reaction rate data on the MY720–DDS system cured isothermally at 177°C: (●) DSC data; (△) OH appearance (FT–IR); (□) ratio of two DDS peaks.

transition temperature of the curing medium approaches the curing temperature. This happens after 140 min of isothermal cure at 140°C. The line width resumes its increase beyond this point. The rate of increase thus represents the rate of cure at or near the zone of vitrification.

160–200°C therefore represents the temperature range at which the primary amine content (22 wt %) is just sufficient to be almost completely consumed just when vitrification would in any event arrest the primary amine–epoxide reaction for samples cured at 177°C. Similar optimal amine content can be calculated for any temperature. Curing process beyond this point is found to be dominated by the epoxide–hydroxyl reaction. The occurrence of this reaction in a vitrified phase is significant because it provides a means to increasing crosslink density of the network without raising the curing temperature and thus risking decomposition. The plot in Figure 11 demonstrates that the rate constant of this process, which consumes approximately 50% of the epoxide at 177°C is more than an order of magnitude smaller than the rate of the epoxide–amine reaction. The exothermicity of this reaction is approximately eight times less than the epoxide–amine reaction, since it evolves 15% of the total heat which is evolved by the MY720–DDS mixture when fully cured. Table IV gives the thermochemical parameters for these two reactions, which have been calculated from the ESR and DSC data.

Application of the Hammond postulate[12] indicates that the epoxide–hydroxyl reaction is likely to have a lower activation energy than the epoxide–primary

TABLE IV
Some Rate Parameters for the TGDDM–DDS Curing System

Process	Rate constant at 177°C	Exothermicity ΔH (J/g)
Epoxide–primary amine	5.5×10^{-4}	~1200
Epoxide–hydroxyl	4.76×10^{-5}	150

amine reaction. This conclusion, if experimentally verified, implies that during B-staging or processing at lower temperatures (120–140°C), the epoxide–hydroxyl reaction will be dominant.

In conclusion, we have provided experimental evidence that the curing process of the TGDDM–DDS system is dominated by certain chemical reactions at certain temperature ranges and conversions. The curing mechanism changes on vitrification, the epoxide–hydroxyl reaction characterized by low activation energy and low exothermicity becoming dominant.

This paper represents the results of one phase of research carried out at the Jet Propulsion Laboratory, California Institute of Technology, under Contract No. NAS7-918, sponsored by the National Aeronautics and Space Administration. We gratefully acknowledge several stimulating discussions with Dr. R. F. Landel and Dr. D. Kaelble.

References

1. F. G. Musatti and C. W. Mascosko, *Polym. Eng. Sci.*, **13**(3), 236 (1973).
2. M. J. Doyle, A. F. Lewis, and H. M. Li, *Polym. Eng. Sci.*, **19**, 687 (1979).
3. J. K. Gillham, *Polym. Eng. Sci.*, **19**, 676 (1979).
4. G. A. Senich and W. J. MacKnight, *Polym. Eng. Sci.*, **19**, 313 (1979).
5. A. F. Lewis, M. J. Doyle and J. K. Gillham, *Polym. Eng. Sci.*, **19**, 683 (1979).
6. D. H. Kaelble, *Am. Chem. Soc., Org. Coat. Appl. Polym. Sci. Proc.*, **46**, 241, 246, 328 (1982).
7. J. B. Enns and J. K. Gillham, *Am. Chem. Soc., Org. Coat. Appl. Polym. Sci. Proc.*, **46**, 592 (1982).
8. M. Cizmecioglu and A. Gupta, Soc. Plast. Ind. 37th Annual Conference of Reinforced Plastics/Composites Conference, Washington, D.C., preprints, Jan. 1982, Paper No. 20E.
9. M. Cizmecioglu and A. Gupta, *SAMPE Q.*, **13**(3), 16 (1982).
10. *Photophysics of Aromatic Molecules*, J. B. Birks, Ed., Wiley-Interscience, New York, 1971.
11. E. T. Mones and R. J. Morgan, *Am. Chem. Soc., Polym. Prepr.*, **22**(2), 249 (1981).
12. E. C. Boozer, G. S. Hammond, C. E. Hamilton, and J. N. Sen, *J. Am. Chem. Soc.*, **77**, 3233 (1955).

Received September 20, 1982
Accepted October 27, 1982